The effect of cortical tension on bleb size and frequency in a mechanically resistive environment

Michael Barile

Spring 2019

1 Introduction

Migrating cells exhibit two primary modes of motility, the first characterized by the well-studied phenomenon of actin-rich protrusions such as pseudopods, filopodia and lamellipodia, the second, and the main concern of this paper, by blebs. Blebs are rounded, pressure-driven protrusions of the cell membrane. They are formed by either an ablation of the cortex, or by local detachment of the membrane from the cortex. In either case, cytosol from the cell interior flows into the region between the cortex and the cell membrane and creates a blister-like bulge. In the initial stages of bleb formation, the membrane is devoid of an underlying actin cortex, but in relatively short order, actin is recruited and a new cortex assembles, coupled to the membrane, while the old cortex degrades into the body of the cell ([1],[2],[10]).

While blebs have long been observed to occur in various cell processes such as cytokinesis and apoptosis (organized cell death) ([12]), in recent years research has been largely focused on their role in cell motility. Cells have been seen to resort to bleb-based movement, as opposed to using actin-based protrusions, when moving through environments of high mechanical resistance ([2],[6]). Cancer cells migrating through dense tissue would be one such example ([1]). Thus, the study of blebs is critical in developing a complete model of cell motility. The advances in understanding blebs have been profound over the last twenty years or so, yet a clear picture of all cellular and environmental factors that regulate bleb formation and growth has been elusive. However, we can say confidently that intracellular pressure is needed to promote membrane expansion and hence bleb growth, and that myosin II, a protein responsible for cortical contraction and tension, is inextricably linked to regulating the intracellular pressure ([11],[12],[13]).

Previous studies have investigated the effects of both cortical tension and mechanically resistive environments in bleb size and frequency ([6],[12]). While these studies offer valuable insights into cellular and environmental factors regulating bleb formation, they have limitations. In [12], cells are subjected to various concentrations of the ROCK inhibitor Y27632, a drug known to reduce myosin II activity and hence cortical tension. Blebs are

then induced via laser ablation of the cortex in a highly controlled laboratory environment, thus allowing cells and blebs to retain a nearly circular shape. A model relating bleb size to cortical tension is then constructed using these underlying geometric assumptions. However, in a natural environment, cells and blebs often have highly irregular boundaries that are not well-approximated by intersecting circles. In [6], *Dictyostelium discoideum* cells are coerced into microfluidic channels offering varying degrees of mechanical resistance. Here, a given cell migrates in isolation from other cells, and thus maintains a dedicated direction of motility dictated by the cAMP gradient. This does not mimic the setting in which cells migrate en masse, where direction of motility is dictated by both a cAMP source and cAMP emitted from neighboring cells ([7]).

In our experimental setup, *Dictyostelium discoideum* cells are treated with blebbistatin, a drug with similar effects to ROCK inhibitor Y27632 in reducing myosin II activity and cortical tension. We then simply allow the natural mechanisms that control bleb formation to go into effect and study bleb size and frequency across the different treatments. In contrast to [12], we do not induce blebs via laser ablation of the cortex. Additionally, cells are not isolated and are therefore allowed to respond to both a cAMP source and cAMP emitted from neighboring cells, unlike [6]. We believe that this setup more accurately mimics migration of *Dictyostelium discoideum* cells in a natural three-dimensional environment.

In addition to studying bleb behavior in cells across treatments of different cortical tensions, we introduce cells containing no talA (talA null cells) into our experimental setup. TalA is one type of tethering protein responsible for membrane-cortex coupling. While changes in bleb frequency in talA null cells have been observed, to our knowledge, no study has been done observing the effects of the absence of talA on bleb size ([4],[14]). By laboratory observation, we postulate that these cells produce smaller blebs. It is an aim of our study to confirm or refute this quantitatively. In the following, it will be seen that talA null cells do indeed produce significantly smaller blebs when compared to a control group. We compare talA null cells across the various blebbistatin treatments to determine if the reduced bleb sizes exhibited by the mutant cells may be a consequence of diminished cortical tension.

We present here a brief outline of the following. In the *Methods* section, we describe laboratory and measurement methods in detail, followed by an overview of all statistical tests employed to determine significant differences in bleb size and frequency across treatments. We then present test results in the *Results* section. Implications of our results are analyzed in the *Discussion* section, and finally, we summarize our study and present possible future areas of investigation in the *Conclusion.*

2 Methods

2.1 Laboratory Methods

Axenically grown wildtype (Ax2) *D. discoideum* cells were treated with the myosin II inhibitor, blebbistatin, at concentrations of 0 μM, 50 μM , 100 μM and 150 μM. Blebbing activity was observed using the under agarose assay presented in [10] with the following modifications. Cyclic AMP competent cells, previously starved and plated onto a 2 well chambered coverglass slide were allowed to crawl under a 0.7% agarose gel in response to 4μM cyclic AMP. Once a noticeable wave of cells was observed under the gel, the media was removed from the side of the slide containing cells as well from the side containing cyclic AMP. The cell side of the slide was replaced with a 100ul mixture of PBM and blebbistatin. The cyclic AMP side of the well was replaced with 200ul mixture of cyclic AMP and blebbistatin. This was done to balance the concentration of blebbistatin across the agarose gel. The cells were allowed to endocytose the drug for 20-30 minutes after which each cell was observed over a 30 second duration. For details on the microscopy see [10]. All images were acquired using a 100x/1.44 oil immersion objective with frame rate of 1.93 seconds and processed in imageJ.

2.2 Bleb Detection and Measurements

After cell images are captured, we set about recording occurrences of blebs in each cell. For a given cell, the sequence of images, captured at time intervals of 1.93 seconds, are compiled into an AVI file using *ImageJ*. Blebs are detected by looking for membrane detachment, which will be seen as a shadow emerging from the cell boundary (Fig. 1). In subsequent frames, we will see actin, marked with a fluorescent green protein, fill the detached membrane. Ultimately, a new actin cortex will form underlying the membrane, and the old actin cortex will fall away into the body of the cell. We are interested in recording what we will call the stable frame of the bleb. To some degree, this is subjective, but we are looking for the frame in which the bleb stops expanding, the new actin cortex has completely formed, and the old cortex is still in its approximately original position (Fig. 2). Such a state is possible because bleb expansion happens at a faster rate then the degradation of the original cortex ([2]).

Occasionally, we will see blebs form without observing the membrane shadow. Since images are taken at regular time intervals, it is possible for the membrane detachment to occur and for a bleb to form between frames. In this case, we look for the same characteristics of the stable frame of the bleb and record. Furthermore, we will observe other protrusions, known as pseudopods, emerging from the cell boundary. These can be distinguished from blebs in that they are rich in actin (Fig. 3). In some instances, after a bleb forms, we will see actin rich protrusions extend from the bleb itself. When we set about measuring bleb area, care must be taken to distinguish between the bleb and any possible actin protrusions extending from the newly formed membrane-cortex complex.

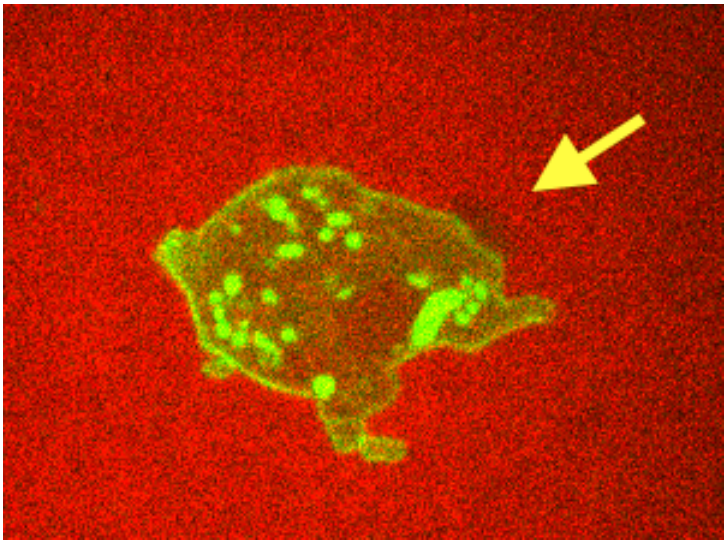

Figure 1: membrane shadow seen in image preceding Fig. 2

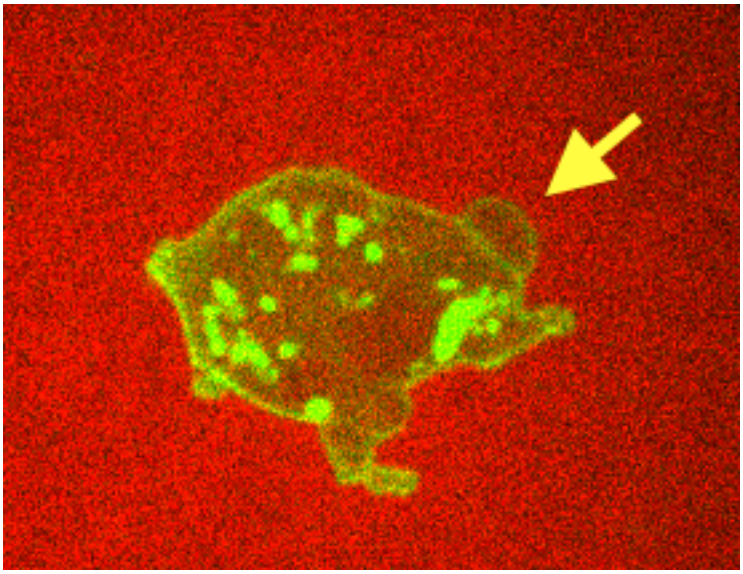

Figure 2: stable frame of bleb

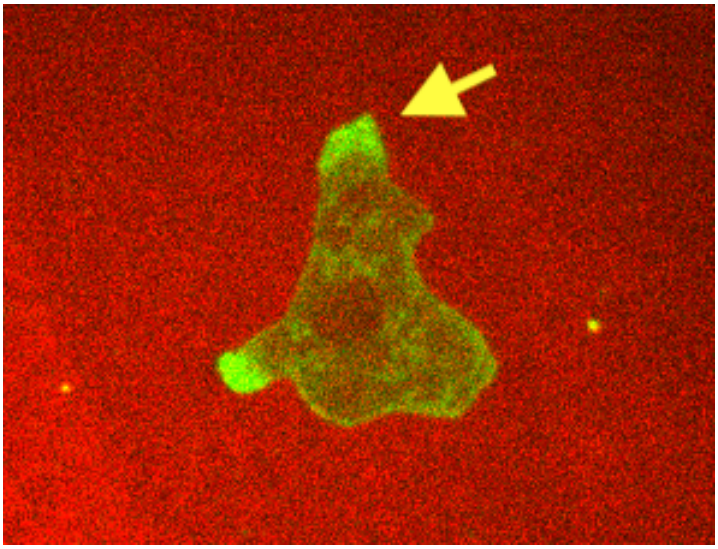

Figure 3: actin-rich protrusion

Cell boundaries are captured and discretized by the process described in [10]. Cell areas of stable frames are then calculated with the same *Mathematica* code used for bleb area calculation, described and included below. To eliminate the potential of rescaling the cell image when performing bleb measurements, the image from which the cell boundary discretization is calculated should be used for bleb images, and we do not crop or permanently alter this image in any way. The cell image is copied directly from the relevant *Mathematica* file where the image processing is performed and brought into a new *Mathematica* notebook file. The cell image is already attached to an underlying cartesian coordinate system, and this underlying coordinate system will copy into the new notebook as well. At this point, we can safely zoom in on the image, without the possibility of rescaling, to get a closer look at the bleb boundary. Using the *Mathematica* coordinates tool, we select points in either a clockwise or counterclockwise direction around the bleb boundary (Fig. 4). These points are copied from the coordinate tool pop-up box and stored in a list. We make use of the following *Mathematica* functions for bleb area calculation and visualization: *BoundaryMeshRegion, TriangulateMesh, Area*. As can be seen in the code below, we are simply connecting our selected boundary points with line segments and using the built-in functions to calculate the enclosed area. This area is recorded, and together with the corresponding cell area, the ratio is calculated.

We include the *Mathematica* code for calculating bleb areas. This code can be easily modified to calculate cell areas as well, where the `blebPoints` list is replaced by `eqlists[[frame number]]`, generated by the methods described in [10].

```
blebPoints = {list containing ordered bleb points};
```

```
list = {}
For[j=1, j ≤ Length[blebPoints], ++j,
AppendTo[list,j]
];
list = AppendTo[list,1];
region = TriangulateMesh[BoundaryMeshRegion[blebPoints, Line[list]]]
blebArea = Area[region];
Print["Area:  ", blebArea]
```

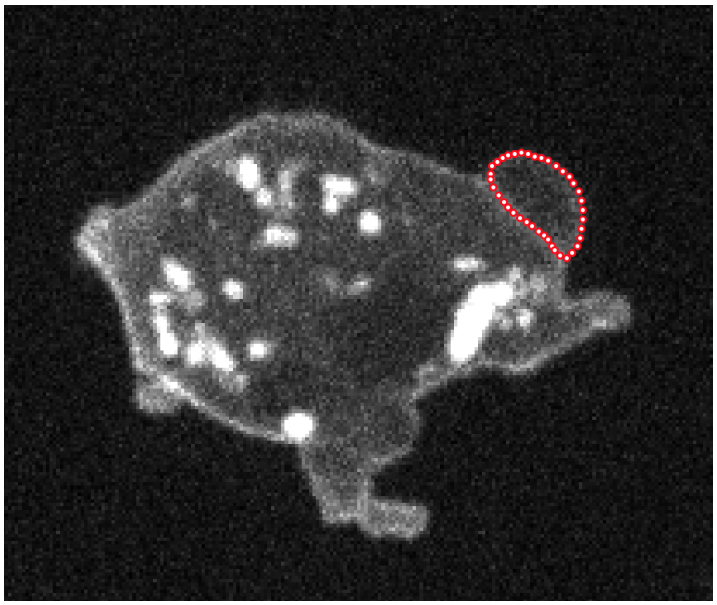

Figure 4: points along bleb boundary

2.3 Statistical Methods

We describe the various statistical tests employed in the analysis of data. The statistical tests are done using *R*. For more detailed derivations, consult [5], [8], [9].

Analysis of Variance (ANOVA)

relevant functions in R: **aov()**, **summary.aov()**, **oneway.test()**

We are interested in knowing if reduced cortical tension and the absence of tal A has an effect on bleb-to-cell area ratio and bleb frequency in *Dictyostelium discoideum* cells under .7% agarose gel. To detect such an effect, we may employ the popular ANOVA

test to determine if there are significant differences across the treatments, provided the assumptions under which the test produces reliable results are satisfied. These assumptions are as follows:

- Observations are independent within and across treatments.
- Residuals are normally distributed.
- The variance in each treatment is the same (homoscedasticity).

Before proceeding, we make several comments about independence of observations within and across treatments, an assumption that must hold for the statistical tests we employ. We will assume independence across treatments. This is a reasonable assumption given the manner in which the experiments were performed. We turn our attention to independence within treatments. Determining independence under our setup is difficult using traditional time series analysis methods. Images are captured using a confocal microscope which exposes the cells to a laser. After about thirty seconds, cells stop exhibiting normal behavior and die. Thus, a particular cell does not produce a significant amount of data with which to determine possible autocorrelation. We instead aim to present a plausible argument for independence of observations within treatments, given the limitations of our experiments.

In [11], a model is constructed to address apparent contradictions in the results of [3] and [12] involving intracellular pressure propagation during blebbing. The authors in [11] indicate that when two blebs are initiated, where the second bleb is initiated at a short time interval after the first, the second bleb is always smaller. Such behavior would certainly indicate dependence of observations. To determine whether this holds under our experimental setup, we record the direction of ratio changes over 193 bleb occurrences. As an example, if the bleb-cell area ratios for a particular cell are $.02, .015, .04, .05, .025$, we record this as $0, 1, 1, 0$, where 0 indicates a decrease in ratio, 1 an increase in ratio. We then simply tally up the results. We find that there is an increase in ratio in 51.2% of occurrences, and a decrease in 48.8% of occurrences. This indicates that if a bleb occurs, the ratio (and hence size, see discussion in *Results* section) generated by the following bleb is essentially equally likely to be larger as it is smaller.

Of course, the above discussion does not demonstrate independence of observations, but it does rule out the problem posed by the model in [11] in our data. For further analysis, we employ a graphical approach. We include two observation vs. residual plots for bleb-cell area ratio from cells in our study (Fig. 5 and Fig. 6). Here, the x-axis represents order of observation, the y-axis residuals, where residual is defined as follows: for a given treatment, let $\hat{y}$ be the average of all observations. Let y_i be the ith observation. Then $r_i = y_i - \hat{y}$ is the ith residual. We visually inspect a number of such observation vs. residual plots for cells in all treatments. It should be emphasized here that the number of observations in each cell is too small to be conclusive, but in absence of any obvious time-related trends

together with the results involving direction of ratio change in our study as described above, we conclude that bleb-cell area ratio observations are independent within cells.

As will be seen in the *Results* section, we will ultimately pool ratios from all cells under a given treatment. We therefore want to provide some check on independence of observations between cells under the same treatment. For instance, under the pure PBM treatment, we want to know if the observations recorded in a particular cell are affected by neighboring cells in the same treatment. We again include an observation vs. residual plot (Fig. 7), this time for bleb-cell area ratios from all cells under a given treatment. The x-axis represents the observation order, the y-axis residuals. We visually inspect the plot for any obvious trends, like a time-dependent drift, patterns of alternating positive and negative residuals, etc. Although this method is somewhat crude, in absence of any clear trend in the scatter plot, we conclude that bleb-cell area ratio observations are independent between cells under the same treatment. We make this assertion for all treatments.

To determine independence of observations for bleb frequency, we include another observation vs. residual plot (Fig. 8). Again, we visually inspect for any possible trends. Observe, the first three residuals decrease in value with each observation, while the fourth-sixth and the seventh-ninth sequences of residuals follow a similar pattern. Given the small number of observations, it is plausible that this pattern occurs purely by chance, but we postulate a possible cause. When the observations are captured, the laser from the confocal microscope excites the medium. This causes cells to round up in shape and eventually die. Since blebs occur more frequently in regions of negative curvature, we would expect rounded cells to bleb less frequently. If, while a cell image is being taken, other cells are within or close to the field of view, they will be exposed to the laser for a prolonged period of time, thus causing them to round up and bleb less frequently. In our case, it is possible that the first three observations were made in this manner, before moving on to a different grouping of cells for observations four-six and seven-nine. As a recommendation for future experiments on bleb frequency, it may be best to randomize the field of view so as to avoid possible complications. This pattern may indicate dependence in observations. For our purposes, as will be seen in the *Results* section, other assumptions will fail to hold for bleb frequency data, so we will ultimately abandon our statistical analysis in this case and simply present our observations visually as trends requiring further investigation.

We now briefly explain the methodology behind ANOVA. We define the *overall mean* as μ, a parameter common to all treatments, and we define the ith *treatment effect*, τ_i, as a deviation from the overall mean where $\sum \tau_i = 0$. Then, under the ANOVA assumptions, we are effectively saying that each treatment is normally distributed with mean $\mu_i = \mu + \tau_i$ and variance σ^2. Our null hypothesis, H_0, and alternative hypothesis, H_1, can be stated:

$$H_0 : \tau_i = 0 \,\forall\, i$$

$$H_1 : \exists\, i \mid \tau_i \neq 0$$

In accordance with convention, we reject the null hypothesis if ANOVA returns a p-value of 0.05 or less. A failure to reject the null hypothesis means there is not sufficient evidence

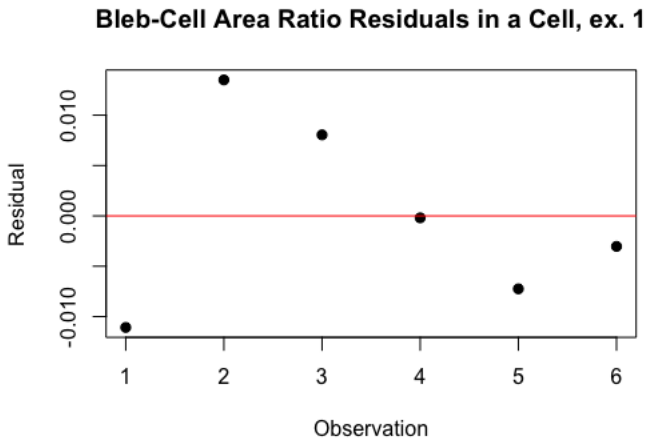

Figure 5: Ratio Residuals for in Cell, ex. 1

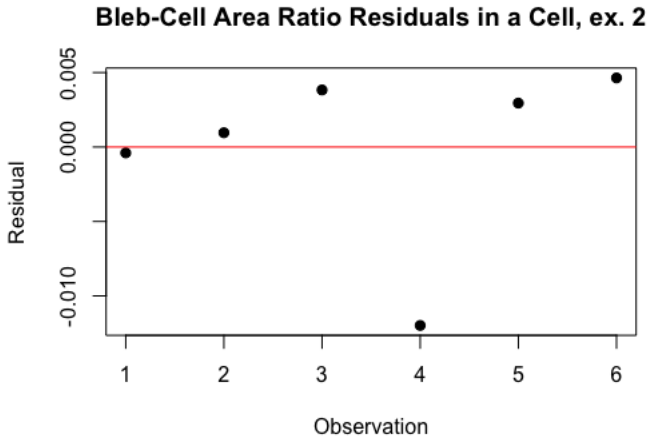

Figure 6: Ratio Residuals in Cell, ex. 2

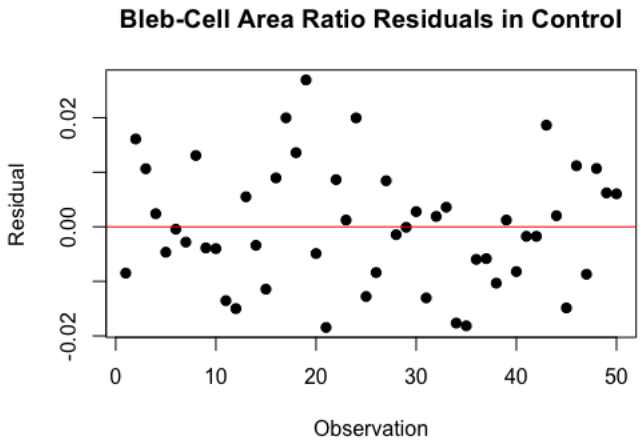

Figure 7: Ratio Residuals in Control

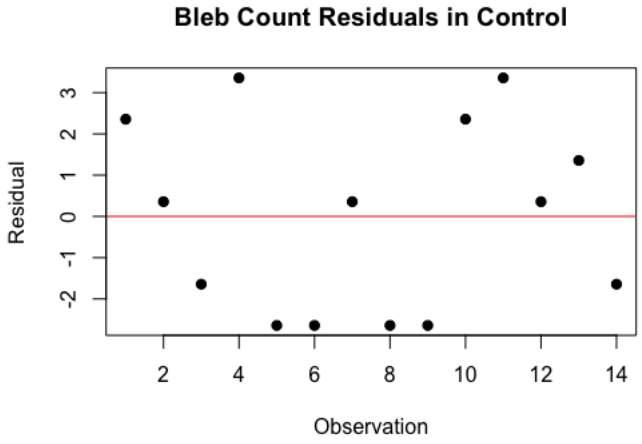

Figure 8: Frequency Residuals in Control

to believe that the alternative hypothesis is true. Thus, given our data, a failure to reject H_0 gives us reason to believe that there is no difference in means across the treatments. However, if ANOVA indicates that we should, in fact, reject H_0, then we accept H_1, and so our data indicates that there is at least one pairwise significant difference in means across treatments. To determine which treatments are exhibiting such differences, we employ Tukey's Honest Significant Difference test, described below.

If our data satisfies normality of residuals, but fails to satisfy equality of variances, we employ the the *oneway.test()* function, a version of ANOVA that gives reliable results while relaxing the homoscedasticity condition.

Levene's test

relevant functions in R: **leveneTest()**

Levene's test is used to assess homogeneity of variances across treatments. Here, the null hypothesis states that each treatment has the same variance. We reject the null hypothesis if Levene's test yields a p-value of 0.05 or less. If, in addition to failing Levene's test, our data fails to satisfy normal distribution of residuals, we attempt to find a transformation that will establish equality of variances and move to a nonparametric approach. However, as described above, if equality of variances fails to hold while the other assumptions of ANOVA are satisfied, we use the *oneway.test()* function.

Shapiro-Wilk test

relevant functions in R: **shapiro.test()**

We employ the Shapiro-Wilk test to determine if residuals are normally distributed. Extreme departures from normality can severely affect the reliability of ANOVA, leading us to adopt non-parametric methods for our hypothesis testing. The null hypothesis of the Shapiro-Wilk test assumes normal distribution of residuals of the model. We reject the null hypothesis if the test yields a p-value of 0.05 or less.

Tukey's Honest Significant Difference test

relevant functions in R: **TukeyHSD()**

If ANOVA returns a p-value of no greater than 0.05, we use the Tukey Honest Significant Difference Test to determine precisely which treatments have significant differences in means. We test all pairwise means comparisons, so if μ_i is the mean of the ith treatment, the null hypothesis and alternative are stated:

$$H_0 : \mu_i = \mu_j$$

$$H_1 : \mu_i \neq \mu_j$$

for all $i \neq j$. The *TukeyHSD()* function in *R* will generate a table containing all p-values associated with pairwise comparisons. We can then easily read off which treatments have significantly differing means, where 0.05 is our significance level.

Kruskal-Wallis test

relevant functions in R: **kruskal.test()**

The Kruskal-Wallis test is the nonparametric counterpart of ANOVA. We use this test when the Shapiro-Wilk test indicates that residuals are not normally distributed. The assumptions of Kruskal-Wallis are as follows:

- Observations are independent within and across treatments.
- The measurement scale is ordinal or greater.
- The populations are identically shaped and scaled.

We use a graphical approach, illustrated in the *Results* section of this paper, along with Levene's test, to check the reasonability of the last assumption. The second assumption is easily seen to be satisfied by the nature of our experiments.

For Kruskal-Wallis, our null hypothesis states that the medians of all treatments are equal. Note the difference with the ANOVA null hypothesis, which asserts that the *means* of all treatments are equal. We reject the null hypothesis if Kruskal-Wallis yields a p-value of less than 0.05 and conclude that at least one pairwise significant difference in medians exists.

Dunn's test

relevant functions in R: **dunn.test()**

Dunn's test is the nonparametric counterpart of Tukey's test. We use Dunn's test provided the Kruskal-Wallis test produces a p-value of no greater than 0.05 to determine which treatments have significant differences in their medians. We use the Benjamini-Hochberg p-value adjustment in the *dunn.test()* function. Analogous to Tukey's test, we compare medians of the treatments, with our null hypothesis asserting that the medians are the same across all pairs of treatments. The *dunn.test()* function will generate a table where we can easily see which treatments have significantly different medians. For pairwise comparisons, we reject the null hypothesis if Dunn's test yields a p-value of no greater than 0.025.

2.4 Results

We first comment on the choice of bleb-cell area ratio as opposed to bleb size as a measure of describing behavior of cells under different treatments. We have included a box plot (Fig. 9), as well as a table of summary statistics for cell area measurements across all treatments. Measurements are in square μm. Observe the large differences in means (summary statistics) and medians (box plot) between some of the treatments, as well as the large standard deviations within treatments. The confocal microscope captures a cross-section of the cell. Since the cells are largely flattened by the agarose gel, we can study them as two-dimensional objects, but they are not entirely two-dimensional. The differences seen in the cell measurements result from a combination of the plane of view of the confocal microscope, as well as differences in sizes between the individual cells. Since a larger cell or larger cellular-cross section will possibly produce larger bleb measurements, a better characterization of bleb size for comparison across treatments is bleb-cell area ratio. As a simple example, suppose cell 1 has an area of 270, while cell 2 has an area of 160. Suppose further that cell 1 produces one bleb with area 8.1, while cell 2 produces one bleb with area 6.7. If bleb area is used as our characterization of blebbing behavior, we will note that cell 1 produces a larger bleb than cell 2 and record the results. However, this approach does not take into account the area of the cellular cross-section. Here, cell 1 in fact produces a smaller bleb size relative to cell size when compared to cell 2, 3% to 4.2%. Thus, to account for differences in area between cells, we employ statistical tests to detect significant differences in bleb-cell area ratio as opposed to bleb size. It should be noted, however, that within a particular cell, the cell area changes minimally for the duration of the imaging. This justifies the statement in the *Methods* section that if a bleb occurs, the size generated by the following bleb is essentially equally likely to be larger as it is smaller, in contradiction to [11].

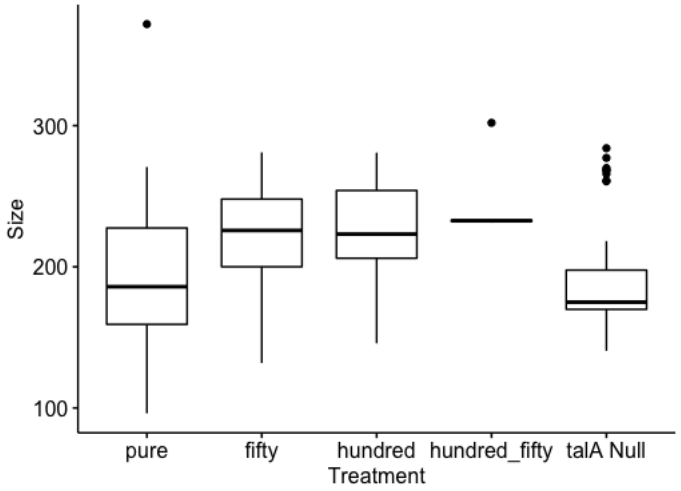

Figure 9: Cell Areas

Summary Statistics Cell Area			
Treatment	*Count*	*Mean*	*SD*
control	50	195	50
50 blebbistatin	49	220	36.5
100 blebbistatin	26	221	44.9
150 blebbistatin	6	244	28.4
talA null	52	191	36.6

All tests are run on treatments under 0.7% agarose gel. For all tests involving bleb size, we look for significant differences across treatments of 50 μM, 100 μM and 150 μM blebbistatin, talA null and a control group. For bleb frequency, we test across 50 μM, 100 μM and 150 μM blebbistatin treatments and the control group.

2.4.1 Maximum Bleb-Cell Area Ratio

In [12], the authors record the maximum bleb-cell area ratio at varying degrees of cortical tension and fit their mathematical model to the observed data. We test for significant differences in maximum bleb-cell area ratio across treatments in our experimental setup by recording the maximum ratio in each cell under a given treatment and executing the appropriate statistical tests.

Summary Statistics Max Ratio			
Treatment	*Count*	*Mean*	*SD*
control	14	0.0318	0.0133
50 blebbistatin	18	0.0259	0.0126
100 blebbistatin	11	0.0306	0.0157
150 blebbistatin	2	0.0230	0.0116
talA null	10	0.0244	0.0129

Levene's test for Homogeneity of Variances	
p-value	0.9538

Shapiro-Wilk normality test	
p-value	0.1887

Since the homogeneity of variances and normal distribution of residuals assumptions are satisfied, we execute ANOVA.

ANOVA	
p-value	0.567

Conclusion: The ANOVA p-value is greater than 0.05, indicating that no significant differences exist across treatments for maximum bleb-cell area ratio.

2.4.2 Average Bleb-Cell Area Ratio

Next, we record the average bleb-cell area ratio in each cell under a given treatment and execute the appropriate statistical tests.

Summary Statistics Average Ratio			
Treatment	*Count*	*Mean*	*SD*
control	14	0.0244	0.00831
50 blebbistatin	18	0.0200	0.00932
100 blebbistatin	11	0.0225	0.00989
150 blebbistatin	2	0.0177	0.00404
talA null	10	0.0152	0.00494

Levene's test for Homogeneity of Variances	
p-value	0.2985

Shapiro-Wilk normality test	
p-value	0.4734

Since the homogeneity of variances and normal distribution of residuals assumptions are satisfied, we execute ANOVA.

ANOVA	
p-value	0.116

Conclusion: The ANOVA p-value is greater than 0.05, indicating that no significant differences exist across treatments for average bleb-cell area ratio.

2.4.3 All Bleb-Cell Area Ratios

We record all bleb-cell area ratios under a given treatment and compare across treatments. Unlike the previous tests, where one observation is used to characterize bleb behavior in a particular cell under a given treatment, we now pool ratios recorded from all cells under each treatment. The advantage of this approach is that it makes use of all of our recorded data and provides a more complete description of the behavior exhibited under each treatment.

Summary Statistics All Ratios			
Treatment	*Count*	*Mean*	*SD*
control	50	0.0261	0.0109
50 blebbistatin	49	0.0202	0.0118
100 blebbistatin	26	0.0248	0.0135
150 blebbistatin	6	0.0196	0.00806
talA null	52	0.0156	0.00886

Levene's test for Homogeneity of Variances	
p-value	0.151

Shapiro-Wilk normality test	
p-value	0.0000

The Shapiro-Wilk test indicates that normal distribution of the residuals is violated, so we can not employ ANOVA and instead turn to its nonparametric counterpart, Kruskal-Wallis. We use a graphical approach, together with Levene's test, to assess the reasonability of the assumption that all populations are identically shaped and scaled (Fig. 10, 11, 12, 13, 14). With the exception of the 150μ blebbistatin treatment, which contains only six observations, all distributions appear to be skewed right. Furthermore, Levene's test

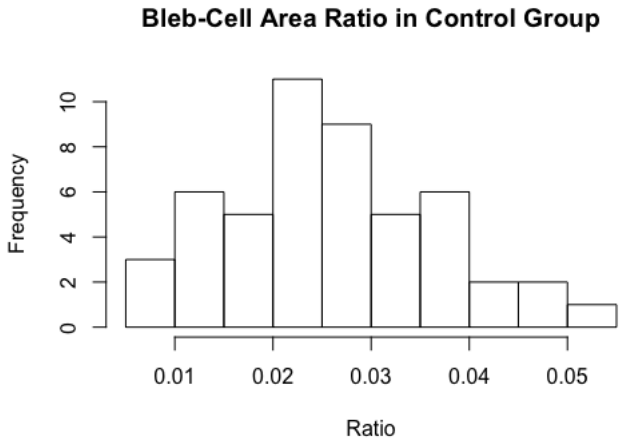

Figure 10: Pure PBM

indicates that we do not have sufficient evidence to believe that homogeneity of variances is violated. While comparisons in the "peaks" of each histogram may pose a problem in our analysis, given the comparatively small sample sizes with which to determine the true shape and scale of the individual distributions, we accept the assumption that the distributions are identically shaped and scaled. We employ Kruskal-Wallis.

Kruskal-Wallis rank sum test	
p-value	0.0000

Kruskal-Wallis yields a p-value of less than 0.05. Thus, significant differences exist across treatments. We use Dunn's test to determine which treatments are exhibiting significant differences.

Dunn's test (p-values)				
	50μM	100μM	150μM	control
100μM	0.1281			
150μM	0.4111	0.3045		
control	0.0066*	0.2402	0.1887	
talA null	0.0424	0.0025*	0.1903	0.0000*

Conclusion: Dunn's test indicates that significant differences exist between the control group and the 50μM blebbistatin treatment, between the control group and talA null, and between talA null and 100μM.

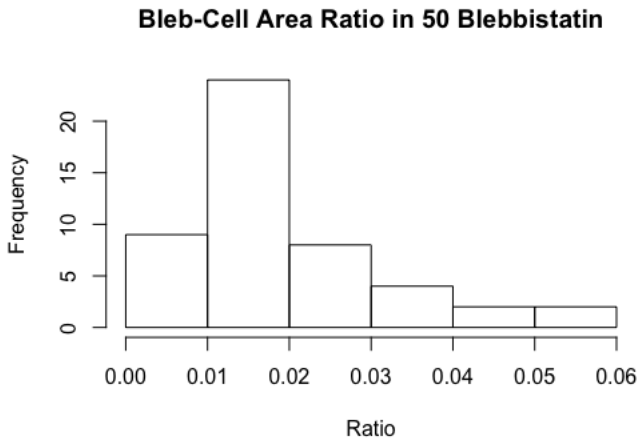

Figure 11: 50 μM blebbistatin

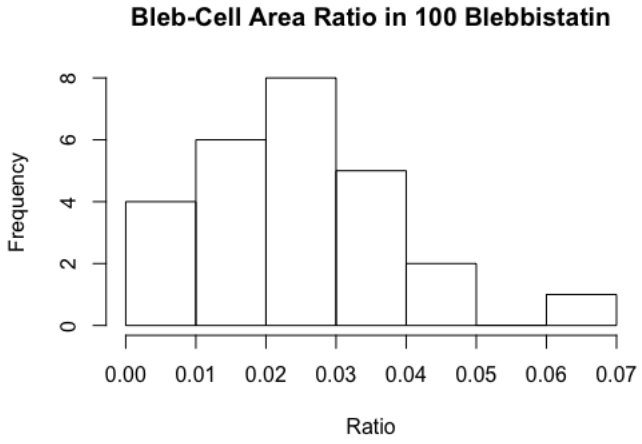

Figure 12: 100 μM blebbistatin

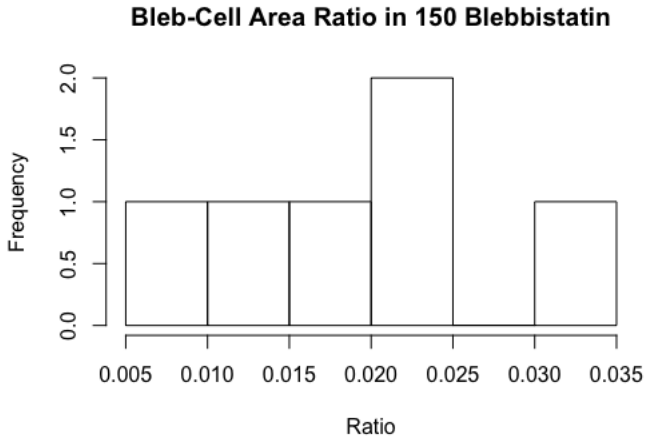

Figure 13: 150 μM blebbistatin

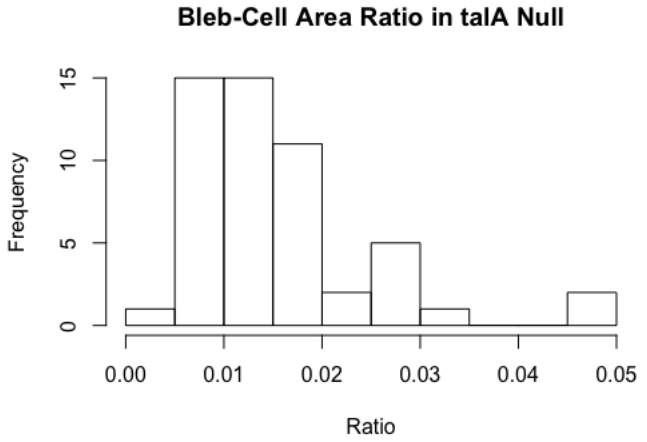

Figure 14: talA null

2.4.4 Bleb Frequency

We record the number of blebs observed in each cell under a given treatment and execute the appropriate statistical tests across all treatments (excluding talA null).

Summary Statistics Bleb Frequency			
Treatment	*Count*	*Mean*	*SD*
control	14	3.57	2.21
50 blebbistatin	18	2.72	1.67
100 blebbistatin	19	1.95	2.63
150 blebbistatin	17	0.353	1.22

Levene's test for Homogeneity of Variances	
p-value	0.03853

Shapiro-Wilk normality test	
p-value	0.0000

We see that both the homogeneity of variances and normality of residuals assumptions are violated, so we can not use ANOVA. We employed several data transformation methods, including square root, cube root, log, reciprocal and arcsin, but were unable to find an appropriate transformation to obtain homogeneity of variances. Because Kruskal-Wallis requires the assumption that all distributions have the same shape and scale, without homogeneity of variances, we can not be confident that the test will provide reliable results. We present a box plot and a mean plot of the data (Fig. 15 and 16).

Conclusion: Graphically, there is a clear trend indicating that cells bleb less under increasing treatments of blebbistatin and hence reduced cortical tension.

2.5 Discussion

We first discuss the results of our experiments across the various blebbistatin treatments and the control group, momentarily delaying comparison with the talA null treatment. In [12], the authors use maximum bleb-cell volume ratio as a way of characterizing bleb behavior in cells across treatments of various cortical tensions. We test for maximum bleb-cell area ratio across treatments under our experimental setup. We find that no significant differences exist across treatments. We present a mean plot of our results (Fig. 17) for inspection. Observe that treatments along the x-axis are arranged in order of increasing cortical tension. This can be compared to figure 4 in [12] as a graphical contrast of our results. It should be noted that the authors in [12] do not claim statistically significant

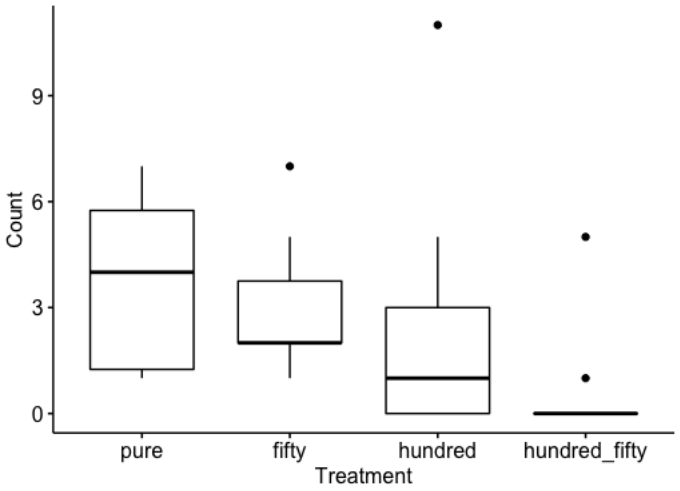

Figure 15: Bleb Frequency Box Plot

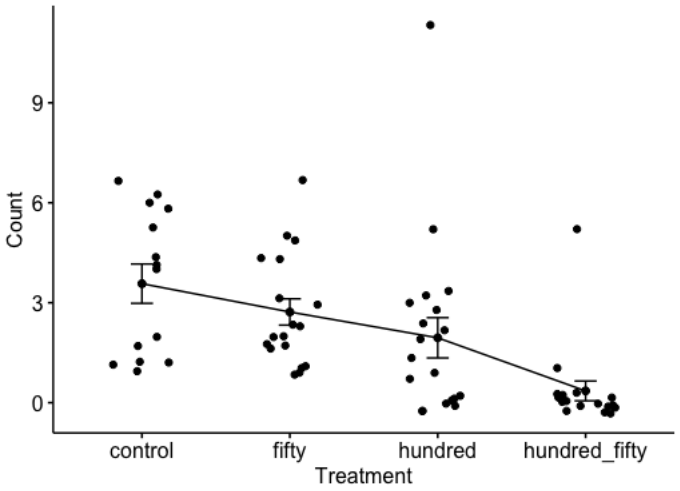

Figure 16: Bleb Frequency Mean Plot

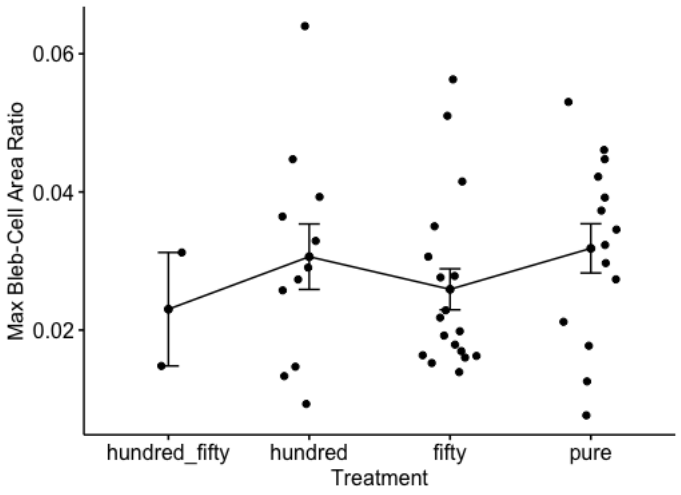

Figure 17: Max Bleb-Cell Area Ratio Mean Plot

differences between treatments. They simply demonstrate graphically that maximum bleb-cell volume ratio decreases with decreasing cortical tension and fit their model accordingly.

One possible explanation of the inconsistency in our results is sample size. We are working with a fairly limited data set, so it is possible that with the addition of more cells, we would see a trend similar to the one exhibited in [12]. It is also possible that even with the addition of more data, the maximum bleb-cell area ratio is not a suitable characterization of bleb behavior to produce statistically significant differences between treatments in our setup. Thus, it may be the case that maximum bleb-cell area ratio is not measurably affected by cortical tension when cells are migrating en masse under 0.7% agarose. An important component of our setup that can not be ignored here is the presence of the agarose gel. Cells are subjected to an increased hydrostatic pressure, which may be a controlling factor in maximum bleb-cell area ratio not present in [12]. It is possible that above a certain threshold of hydrostatic pressure, the effects of this pressure dominate those of cortical tension, thus allowing maximum bleb size to be achieved regardless of treatment.

Another possible factor explaining the inconsistency in our results is purely geometric. In [12], blebs are artificially nucleated by cortical ablation with a laser and retain a spherical shape. Hence, all cross sections of cells are circles. In our experimental setup, the cellular cross sections exhibit highly irregular boundaries. It is possible that geometric properties of the cell boundary play a controlling factor in bleb-cell area ratio in general, and maximum bleb-cell area ratio in particular. In any case, the maximum ratio ignores much of the information produced by a particular cell, so it is plausible that inclusion of all measurements from a cell will be needed to more fully demonstrate differences in bleb-cell

area ratio across treatments, if such differences do, in fact, exist. With this consideration as our motivation, we move on to additional tests.

We test for significant differences in average bleb-cell area ratio across treatments. Our test fails to produce any significant differences. While using the average implicitly takes into account all measurements within a particular cell, we are still left with only one observation per cell with which to perform our tests, again leaving us with a small sample size. Ultimately, we pool our measurements from each cell under a given treatment. By doing this, we dramatically increase our sample size and use all measurements explicitly in our statistical tests. The biggest potential drawback in this procedure is the question of independence of observations, discussed extensively in section 2.3. Employing Kruskal-Wallis and Dunn's test, we observe a significant difference between control and the 50μM blebbistatin treatment, where bleb-cell area ratio is smaller in the 50μM treatment (see summary statistics, section 2.4.3). However, we do not see significant differences between control and any other blebbistatin treatment, or pairwise between each blebbistatin treatment.

The significant difference between control and 50μM blebbistatin treatment gives us some evidence that reduced cortical tension does, in fact, produce smaller bleb-cell area ratios. Observe that we have bleb counts of fifty and forty-nine in the control group and the 50μM blebbistatin treatment respectively, so our sample size is large enough to lend some credence to our results. However, the question remains as to why we are not seeing such differences in any other case, and the cause may again be sample size. The 150μM blebbistatin treatment contains only six observations, and so it is not reliable for comparison, while the 100μM treatment contains twenty-six observations, about half the number of observations in the control group.

Another possible cause for lack of significant differences between treatments other than control and 50μM blebbistatin highlights a limitation of our study, namely the inability to precisely control the gradient of the cAMP source, shown in [6] to have measurable effects on both bleb size and frequency. We elaborate on this limitation at the end of this section, and discuss possible improvements to our experimental design in the *Conclusion*.

In the case of bleb frequency, we can not apply our statistical tests due to violation of assumptions (see section 2.4.4). However, a clear trend is evident (Fig. 16), where cells tend to bleb less under higher concentrations of blebbistatin and hence reduced cortical tension. There is no analog for this observation in [12], but our results are consistent with those found in [6], where the authors demonstrate that inhibition of myosin II activity due to blebbistatin leads to a decrease in bleb frequency.

Finally, we include the talA null treatment in our analysis. From Dunn's test (section 2.4.3), we observe significant differences in bleb-cell area ratio between the control group and talA null, as well as the 100μM blebbistatin treatment and talA null. In the first case, note that there are fifty observations in the control group and fifty-two observations in the talA null treatment, so our sample size is fairly large. The result of the statistical test thus appears to confirm the laboratory observation that talA null cells produce smaller blebs. In the second case, it is again possible that the results are affected by the relatively

small number of observations in the 100μM blebbistatin treatment, one half of the number observed in the talA null treatment. Of particular importance is the absence of a significant difference between the 50μM blebbistatin treatment and talA null. Here, we have forty-nine observations in 50μM vs. fifty-two observations in talA null, a reasonable sample size from which to draw conclusions. The lack of a significant difference between these treatments suggests that talA null cells may have diminished cortical tension in line with the cortical tension exhibited by cells in the 50μM blebbistatin treatment. We discuss this further in the *Conclusion*.

We now discuss a limitation in our experimental setup, and the possible effect of this limitation on our results. In [6], the authors demonstrate that bleb size and frequency are affected by the strength of the cAMP gradient. Specifically, a stronger gradient produces larger and more frequent blebs. The experiment in [6] uses microfluidic channels, a setup which allows for precise control of the cAMP source gradient. Our experiment does not allow for such precision, which leaves our results open to the question of variability of the cAMP gradient across treatments. Recall that there exists no significant difference in bleb-cell area ratio between the control group and the 100μM blebbistatin treatment, while comparison of the control group with the 50μM blebbistatin treatment yields a significant difference. The control-50μM result is consistent with [6], while the control-100μM result is not. We suggest two possible causes for this inconsistency, the first being the comparatively small number of observations in the 100μM treatment as discussed above, and the second, a stronger cAMP gradient throughout this treatment that offsets the potential effect of diminished cortical tension in governing the magnitude of bleb-cell area ratio. However, our results concerning bleb frequency are consistent with [6], which gives us some evidence that the potential variability in the strength of the cAMP gradient across treatments is not overriding the effects of cortical tension. While we can not speak definitively without more data, this suggests that the small number of observations in the 100μM blebbistatin treatment is more likely the cause of the inconsistency in our results.

2.6 Conclusion

In summary, we tested for the effects of cortical tension on bleb-cell area ratio and bleb frequency across treatments of varying cortical tension for *Dictyostelium discoideum* cells migrating en masse under 0.7% agarose gel in the presence of a cAMP source. In the case of maximum bleb-cell area ratio, we showed that our results are inconsistent with those found in [12] and discussed possible causes for this inconsistency. For pooled bleb-cell area ratios, our experiment yielded results that were consistent in part with those found in [6]. We again postulated possible causes of inconsistencies in our results. Our bleb frequency results were consistent with those found in [6]. We then showed that talA null cells produce a smaller bleb-cell area ratio when compared to a control group, confirming laboratory observation, and demonstrated that possible reduced cortical tension in these mutant cells may be a cause. We discussed a limitation in our experimental setup due to

the inability to precisely control the cAMP gradient and the possible effect of this limitation on our results. Additionally, we presented a procedure with which to visually identify blebs using *ImageJ*, as well as a method for measuring cell and bleb area in *Mathematica*, and we have included a description of all statistical tests as well as relevant functions in *R* for executing these tests.

We suggest an improvement in our experimental design. We are interested in studying the effects of cortical tension on bleb-cell area ratio and frequency in *Dictyostelium discoideum* cells migrating en masse in a natural three-dimensional environment. In [6], cells are studied in isolation migrating through microfluidic channels and thus have a dedicated direction of motility dictated by the cAMP gradient, where the gradient may be precisely controlled across all treatments. We propose a modification of this setup by widening the channels through which the cells migrate, thereby allowing group migration. This will serve the purpose of mimicking the natural group migration environment, while also allowing for precise control of the cAMP gradient, thereby eliminating a limitation of our experiment. Studying the effects of cortical tension on bleb size and frequency under this setup will yield important results that more accurately characterize bleb behavior of cells in their natural state of motility.

Finally, we believe our study provides strong motivation for the measurement of cortical tension in talA null cells, as well as comparison of this measurement with measurements of cortical tension in cells across various treatments of blebbistatin. While our study has produced some evidence that talA null cells may indeed exhibit reduced cortical tension, it is possible that other factors controlling bleb-cell area ratio are present in talA null cells. Measurement of cortical tension in talA null cells will thus provide important insights in this matter, and may point to additional mechanisms by which cells regulate bleb behavoir.

References

[1] G. Charras and E. Paluch. Blebs lead the way: how to migrate without lamellipodia. *Perpectives*, 9:730–736, 2008.

[2] G. T. Charras, C.-K. Hu, M. Coughlin, and T. J. Mitchison. Reassembly of contractile actin cortex in cell blebs. *The Journal of Cell Biology*, 175(3):477–490, 2006.

[3] G. T. Charras, J. C. Yarrow, M. A. Horton, L. Mahadevan, and T. Mitchison. Non-equilibration of hydrostatic pressure in blebbing cells. *Nature*, 435:365–369, 2005.

[4] C. A. Copos, S. Walcott, J. C. del Alamo, E. Bastounis, A. Mogilner, and R. D. Guy. Mechanosensitive adhesion explains stepping motility in amoeboid cells. *Biophysical Journal*, 112:2672–2682, June 2017.

[5] W. W. Daniel. *Applied Nonparametric Statistics*. Duxbury, 1990.

[6] M. Ibo, V. Srivastava, D. N. Robinson, and Z. R. Gagnon. Cell blebbing in confined microfluidic environments. *PLOS ONE*, 2016.

[7] P. D. Langridge and R. R. Kay. Blebbing of *Dictyostelium* cells in response to chemoattractant. *Experimental Research*, 312:2009–2017, 2006.

[8] D. C. Montgomery. *Design and Analysis of Experiments*. Wiley, fifth edition, 2001.

[9] D. C. Montgomery, G. C. Runger, and N. F. Hubele. *Engineering Statistics*. Wiley, third edition, 2006.

[10] Z. Santiago, J. Loustau, D. Meretzky, D. Rawal, and D. Brazill. Advances in geometric techniques for analyzing blebbing in chemotaxing *Dictyostelium* cells. *PLOS ONE*, 2019.

[11] W. Strychalski and R. D. Guy. Intracellular pressure dynamics in blebbing cells. *Biophysical Journal*, 110:1168–1179, March 2016.

[12] J.-Y. Tinevez, U. Schulze, G. Salbreux, J. Roensch, and J.-F. Joanny. Role of cortical tension in bleb growth. *PNAS*, 106(44), 2009.

[13] K. Yoshida and T. Soldati. Dissection of amoeboid movement into two mechanically distinct modes. *Journal of Cell Science*, 119:3833–3844, 2006.

[14] E. Zatulovskiy, R. Tyson, T. Bretschneider, and R. R. Kay. Bleb-driven chemotaxis of *Dictyostelium* cells. *The Journal of Cell Biology*, 204(6):1027–1044, 2014.